Mathematical Geology, Vol. 34, No. 4, May 2002 (© 2002)

Three-Dimensional Modeling of Mass Transfer in Porous Media Using the Mixed Hybrid Finite Elements and the Random-Walk Methods[1]

H. Hoteit,[2] R. Mose,[2,4] A. Younes,[3] F. Lehmann,[2] and Ph. Ackerer[2]

A three-dimensional (3D) mass transport numerical model is presented. The code is based on a particle tracking technique: the random-walk method, which is based on the analogy between the advection–dispersion equation and the Fokker–Planck equation. The velocity field is calculated by the mixed hybrid finite element formulation of the flow equation. A new efficient method is developed to handle the dissimilarity between Fokker–Planck equation and advection–dispersion equation to avoid accumulation of particles in low dispersive regions. A comparison made on a layered aquifer example between this method and other algorithms commonly used, shows the efficiency of the new method. The code is validated by a simulation of a 3D tracer transport experiment performed on a laboratory model. It represents a heterogeneous aquifer of about 6-m length, 1-m width, and 1-m depth. The porous medium is made of three different sorts of sand. Sodium chloride is used as a tracer. Comparisons between simulated and measured values, with and without the presented method, also proves the accuracy of the new algorithm.

KEY WORDS: mass transport modeling, advection–dispersion equation, random-walk method, laboratory model.

INTRODUCTION

The first generation of groundwater quality models was based on classical techniques, such as finite difference or finite element methods (see, e.g., Kinzelbach, 1986; Pinder and Gray, 1977). These models are used widely, despite the well-known fact that they suffer from numerical diffusion at high grid Peclet numbers and also when the flow is not parallel to the mesh. Seeing the poor results produced

[1]Received 22 September 2000; accepted 27 June 2001.

[2]Institut de Mécanique des Fluides et des Solides, Université Louis Pasteur de Strasbourg, UMR CNRS 7507, 2, Rue Boussingault, F-67000 Strasbourg, France.

[3]Faculté des Sciences et Techniques, Département Physique et Mécanique, 15 Avenue R. Cassin, B.P. 7151, 97715 St Denis Cedex 09, France.

[4]Now at Ecole Nationale du Génie de l'Eau et de l'Environnement de Strasbourg, Quai Koch-B.P. 1039, F-67070 Strasbourg Cedex.

by the codes based on those methods, we have developed a three-dimensional (3D) mass transport model based on the random-walk method. Particle tracking models are free from numerical diffusion, but one must be very careful when developing a code based on the random walk especially when the code is used in heterogeneous media.

The random-walk model has been developed to be used mostly when the advection–dispersion equation is strongly advection dominated. This means that special care must be given to the accuracy of the flow field resolution and then an efficient method must be used for particle velocity calculation and advective displacement computing. Therefore, we present in the first part the numerical model used for the resolution of the flow. Then we recall that a dissimilarity is now well known between the Fokker–Planck equation and the advection–dispersion equation. If we do not consider this dissimilarity, we will have an accumulation of particles in low dispersive regions. Several authors (Ackerer, 1985; Cordes, Daniels, and Rouve, 1991; Labolle, Fogg, and Tompson, 1996; Labolle, Quastel, and Fogg, 1998; Uffink, 1983) have already suggested algorithms to overcome this problem. The assessment of these algorithms has shown that they are not satisfactory. In this paper a new efficient method is presented to avoid this particle accumulation.

In the last part of the paper, we present the simulation of a 3D tracer experiment performed on a laboratory model. This simulation shows the absolute necessity of using the presented algorithm in heterogeneous media.

THE FLOW MODEL

The velocity field is calculated by a mixed hybrid finite element model (Brezzi and Fortin, 1991; Raviart and Thomas, 1977). Because the mixed hybrid finite element method (MHFEM) is not well known in the hydrogeology community, we present briefly in the following the basis of this approximation. The flow of an incompressible fluid in porous media is described by

$$s\frac{\partial H}{\partial t} - \nabla \cdot (\mathbf{K} \cdot \nabla H) = Q_s \tag{1}$$

associated with initial, Dirichlet, and Neumann boundary conditions, where s is the specific storage coefficient (L^{-1}), H the piezometric head (L), $\mathbf{K}$ the hydraulic conductivity tensor (LT^{-1}), and Q_s the source/sink term (T^{-1}).

The MHFEM consists in a simultaneous approximation of the piezometric head H and the specific flux $\mathbf{q} = -\mathbf{K} \cdot \nabla H$, called the Darcy's velocity. The domain is discretized into parallelepipedic elements. On each element E, H and $\mathbf{q}$ are approximated by (Chavent and Roberts, 1991)

- H_E, the mean of the piezometric head in the element E;
- $\mathrm{TH}_{E,i}$, the mean of the piezometric head on each side of E;
- $\mathbf{q}_E$, the vector defined in the element.

We use the Raviart–Thomas space of lower order as a fundamental approximation space over the domain. For an element E of ns sides A_i, the vectorial basis functions $\mathbf{w}_i$ of this space are defined by the following equation:

$$\int_{A_i} \mathbf{w}_i \cdot \mathbf{n}_{E,j}\, dA = \delta_{ij} \quad \text{for } j = 1, \ldots, \text{ns} \tag{2}$$

where δ_{ij} is the Kronecker symbol; $\mathbf{n}_{E,j}$ is the normal unit vector to the edge A_j; and ns $= 6$ for parallelepipedic elements. The velocity $\mathbf{q}_E$ is completely determined by the knowledge of the fluxes $Q_{E,i}$ through each side A_i:

$$\mathbf{q}_E = \sum_{j=1}^{\text{nf}} Q_{E,i} \mathbf{w}_j \tag{3}$$

where $Q_{E,i}$ are considered positive for outflow. The velocity vector is approximated with vector basis functions that are piecewise linear along all coordinate directions. Therefore the basis property (2) completely determines $\mathbf{w}_i$ (Fig. 1). Moreover they verify

$$\int_E \nabla \cdot \mathbf{w}_i\, dV = \sum_{j=1}^{\text{ns}} \int_{A_j} \mathbf{w}_i \cdot \mathbf{n}_{E,j}\, dA = 1 \tag{4}$$

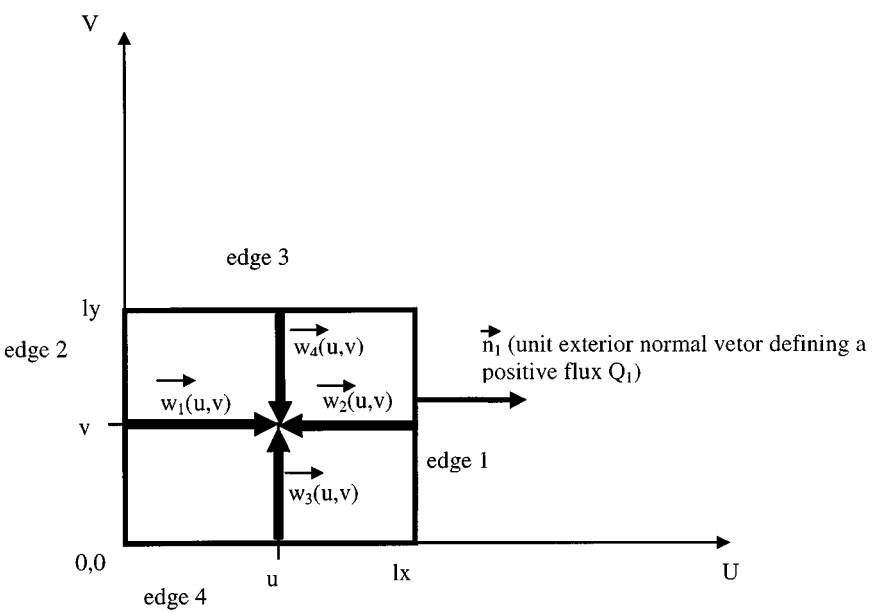

Figure 1. The Raviart–Thomas basis functions of a parallelepipedic element of size $lx \times ly \times lz$ projected on the plan (**O**, *U*, *V*).

The MHFEM ensures an exact mass balance over each element, it gives a velocity throughout all the domain, and the normal component of the velocity is continuous across the interelement boundaries.

Discretization of Darcy's Law

The Darcy's law is written as

$$\mathbf{K}_E^{-1}\mathbf{q}_E = -(\nabla H) \tag{5}$$

This equation is written in a variational form using $\mathbf{w}_i$ as test functions. This leads to

$$\begin{aligned}\int_E \left(\mathbf{K}_E^{-1}\mathbf{q}_E\right)\mathbf{w}_i \, dV &= -\int_E (\nabla H)\cdot \mathbf{w}_i \, dV \\ &= H_E \int_E \nabla\cdot \mathbf{w}_i \, dV - \sum_{j=1}^{\mathrm{ns}} \mathrm{TH}_{E,j} \int_{E,j} \mathbf{w}_i \cdot \mathbf{n}_{E,j} \, dA \end{aligned} \tag{6}$$

Using the properties (2) and (4) of the vectorial functions $\mathbf{w}_i$, we get

$$\sum_{j=1}^{\mathrm{ns}} B_{E,i,j} Q_{E,j} = H_E - \mathrm{TH}_{E,i} \tag{7}$$

where

$$B_{E,i,j} = \int_E \mathbf{w}_i \cdot \mathbf{K}_E^{-1} \cdot \mathbf{w}_j \cdot dV. \tag{8}$$

Fluxes over each side are given by

$$Q_{E,i} = \alpha_{E,i} H_E - \sum_{j=1}^{\mathrm{ns}} B_{E,i,j}^{-1} \mathrm{TH}_{E,j} \quad \text{where } \alpha_{E,i} = \sum_{j=1}^{\mathrm{ns}} B_{E,i,j}^{-1} \tag{9}$$

Discretization of the Mass Balance Equation

The mass balance equation is discretized using a finite volume formulation in space

$$\int_E s \frac{\partial H}{\partial t} \, dV + \int_E \nabla\cdot(\mathbf{q}_E) \, dV = \int_E Q_\mathrm{s} \, dV \tag{10}$$

and an implicit finite difference scheme in time

$$|E| s_E \frac{H_E^n - H_E^{n-1}}{\Delta t} + \sum_{i=1}^{\mathrm{ns}} Q_{E,i}^n = \int_E Q_\mathrm{s}^n \, dV \tag{11}$$

To find the 13 unknowns (H_E, $\mathrm{TH}_{E,i}$, $Q_{E,i}$), we use the variational Darcy's law (9) and the continuity equation (10). To obtain one equation with $\mathrm{TH}_{E,i}$ as unknowns, we also use the continuity properties of piezometric heads and fluxes between two adjacent elements E and E'.

$$\mathrm{TH}_{E,i} = \mathrm{TH}_{E',i} \quad \text{and} \quad Q_{E,i} + Q_{E',i} = 0 \tag{12}$$

All these relations give a system of equations which can be solved by using TH_i as main unknowns (Chavent and Roberts, 1991).

The interest of this mixed formulation is twofold. First, velocity and piezometric heads are obtained simultaneously with the same order of convergence. Second, in the presence of a full permeability tensor, the mixed formulation allows the calculation of the flux at the element level without any problem. On the other hand, finite differences do not allow one to calculate simply these fluxes. Moreover, comparisons between the MHFEM and other methods such as finite differences and finite element methods have shown the superiority of the mixed hybrid approximation especially in heterogeneous media (Mosé and others, 1994; Semra, 1994).

THE MASS TRANSPORT MODEL

In porous media, the mass transport equation is described by the classical advection–dispersion equation which can be written as (Bear, 1979)

$$\frac{\partial C}{\partial t} = -\nabla(\mathbf{U}C) + \nabla(\mathbf{D}\nabla C) \tag{13}$$

where C is the concentration (ML^{-3}), $\mathbf{U}$ the mean pore velocity vector (ML^{-1}), and $\mathbf{D}$ the dispersion tensor ($\mathrm{L}^2\mathrm{T}^{-1}$).

Two approaches of different nature (eulerien and lagrangien) are generally used for the resolution of this equation. In this paper we address a lagrangien method, the random walk. This method is issued from stochastic physics (Fokker, 1914; Planck, 1917, in Gardiner, 1985), and has been used in analysis of diffusion processes. Generally, it is defined as the movement of a particle which undergoes a displacement that partially depends on chance.

Preliminary

The mass transport in porous media may be described by a macroscopic driving force, advection, on which some random fluctuations are added. The random fluctuations are due to the velocity variations around the average velocity in correlation with permeability variations of the porous matrix observed at a macroscopic scale. The theory of stochastic differential equations (Itô, 1951) treats these fluctuations in a certain mathematical idealization.

For sake of simplicity, we consider the one-dimensional problem and a randomly moving particle. We denote by X the position of this particle at a given time. We choose a discrete set of times t_i with constant time step Δt. The impact of the driving force and the fluctuating forces can be described by

$$\Delta X(t_i) = U(X(t_{i-1}))\Delta t + Z(t_i) \tag{14}$$

where $\Delta X(t_i) = (X(t_i) - (X(t_{i-1})$, U is the mean pore velocity (LT^{-1}), and $Z(t_i)$ the random fluctuations. We assume that the average of Z, denoted $\langle Z(t_i)\rangle$, is equal to 0. Otherwise Z would contain a part which acts in a coherent fashion and could be added to the driving force. We assume that the fluctuations at different times t_i and t_j are uncorrelated. Therefore we may postulate that

$$\langle Z(t_i)Z(t_j)\rangle = \delta_{ij} \cdot M \cdot \Delta t \tag{15}$$

where δ_{ij} is the Kronecker symbol which expresses the statistical independence of Z at times t_i and t_j and M is a measure of the size of the fluctuations, equal to 2D, where D refers to the dispersion coefficient.

In a nonuniform field (which implies that D is a function of X), an important question arises concerning at which time the variable X in D must be taken (e.g. Gardiner, 1985). According to Itô's definition, D is governed by the value of X before the jump. On the other hand, in Stratonovitch's definition, D is evaluated at the point halfway through the time interval, that is $D = D(X([t_i + t_{i+1}]/2))$ which is closer to the reality, with fluctuations going on all the time. The Stratonovitch's scheme is difficult to compute, and consequently, the Itô's scheme is quite widely used. The stochastic differential equation is then the following (Itô, 1951):

$$X(t_i) = X(t_{i-1}) + U(X(t_{i-1}))\Delta t + z\sqrt{2D(X(t_{i-1}))\Delta t} \tag{16}$$

where z is a random number issued from a Gaussian distribution with zero mean and unit variance.

It has been shown that this equation is equivalent to the Fokker–Planck equation:

$$\frac{\partial W}{\partial t} = -\nabla(UW) + \Delta(DW) \tag{17}$$

where W is the probability density of the variable $X(t)$. Equation (17) can be written as

$$\frac{\partial W}{\partial t} = -\nabla(UW) + \nabla(D\nabla W) + \nabla(\nabla DW) \tag{17 ter}$$

To be equivalent to the transport equation (13), a term has to be added to the driving force:

$$\frac{\partial W}{\partial t} = -\nabla((U + \nabla D)W) + \Delta(DW) \tag{17 bis}$$

which is exactly the Fokker–Planck equation with U replaced by $U^* = U + \nabla D$.

The equivalent stochastic differential equation to the advection–dispersion equation is then the following:

$$X(t_i) = X(t_{i-1}) + U^*(X(t_{i-1}))\Delta t + z\sqrt{2D(X(t_{i-1}))\Delta t} \tag{18}$$

where $U^* = U + \frac{\partial D}{\partial X}$, which can be replaced by

$$X(t_i) = X(t_{i-1}) + U^*(X(t_{i-1}))\Delta t + z\sqrt{6D(X(t_{i-1}))\Delta t} \tag{19}$$

where z is a random number issued from a uniform distribution between -1 and 1 (as shown by Uffink, 1990).

The additional term $\partial D/\partial X$ is due to the dissimilarity between the Fokker–Planck and advection–dispersion equation. The physical meaning of this term is the conservation of particle flux due to dispersion between two points of space where flow velocities are different. In other words, neglecting this term would yield an abnormal accumulation of particles in low dispersive regions. Inside one element where the velocity field is smooth (and hence dispersion D), the particles will be moved according to the modified Fokker–Planck equation (i.e. U^* instead of U); at the boundary between two elements, where the velocity field, and hence the dispersion is discontinous, the term ∇D cannot be evaluated and we shall propose a new direct treatment of the movement of the particles.

The Fokker–Planck Approach in Three Dimensions for a Smooth Dispersion Tensor

The 3D formulation of the modified Fokker–Planck equation is equivalent to (13) in the case of a smooth dispersion tensor; it is given by

$$\frac{\partial W}{\partial t} = -\sum_{i=1}^{3} \frac{\partial}{\partial X_i}(U_i^* W) + \sum_{i=1}^{3}\sum_{j=1}^{3} \frac{\partial^2}{\partial X_i \partial X_j}(D_{ij} W) \tag{20}$$

where W is the probability density of the variable $X(t)$ and

$$U_i^* = U_i + \sum_{j=1}^{3} \frac{\partial D_{ij}}{\partial X_j}$$

D_{ij} are the elements of the 3D symmetrical dispersion tensor. Their general expression are given by (Bear, 1979)

$$D_{ij} = \alpha_T |U| \delta_{ij} + (\alpha_L - \alpha_T) U_i U_j / |U| \tag{21}$$

where δ_{ij} is the Kronecker symbol ($\delta_{ij} = 1$ if $i = j$ and $\delta_{ij} = 0$ if $i \neq j$); α_{L} is the longitudinal dispersivity component; and α_{T} is the transversal dispersivity component.

The 3D expressions of the displacement components of a particle of tracer are the following:

$$\begin{aligned}
X(t+\Delta t) &= X(t) + U_x^* \Delta t + \left(z_1 \sqrt{6D_{\mathrm{L}}} \frac{U_x}{|U|} - z_2 \sqrt{6D_{\mathrm{T}}} \frac{U_y}{U_{xy}} \right. \\
&\quad \left. - z_3 \sqrt{6D_{\mathrm{T}}} \frac{U_z}{|U|} \frac{U_x}{U_{xy}} \right) \sqrt{\Delta t} \\
Y(t+\Delta t) &= Y(t) + U_y^* \Delta t + \left(z_1 \sqrt{6D_{\mathrm{L}}} \frac{U_y}{|U|} + z_2 \sqrt{6D_{\mathrm{T}}} \frac{U_x}{U_{xy}} \right. \\
&\quad \left. - z_3 \sqrt{6D_{\mathrm{T}}} \frac{U_z}{|U|} \frac{U_y}{U_{xy}} \right) \sqrt{\Delta t} \\
Z(t+\Delta t) &= Z(t) + U_z^* \Delta t + \left(z_1 \sqrt{6D_{\mathrm{L}}} \frac{U_z}{|U|} + z_3 \sqrt{6D_{\mathrm{T}}} \frac{U_{xy}}{|U|} \right) \sqrt{\Delta t}
\end{aligned} \tag{22}$$

where

$$|U| = \sqrt{U_x^2 + U_y^2 + U_z^2} \quad \text{and} \quad U_{xy} = \sqrt{U_x^2 + U_y^2} \tag{23}$$

$$\begin{aligned}
U_x^* &= U_x + \frac{\partial D_{xx}}{\partial X} + \frac{\partial D_{xy}}{\partial Y} + \frac{\partial D_{xz}}{\partial Z} \\
U_y^* &= U_y + \frac{\partial D_{yx}}{\partial X} + \frac{\partial D_{yy}}{\partial Y} + \frac{\partial D_{yz}}{\partial Z} \\
U_z^* &= U_z + \frac{\partial D_{zx}}{\partial X} + \frac{\partial D_{zy}}{\partial Y} + \frac{\partial D_{zz}}{\partial Z} \\
D_{\mathrm{L}} &= \alpha_{\mathrm{L}} |U| \\
D_{\mathrm{T}} &= \alpha_{\mathrm{T}} |U|
\end{aligned} \tag{24}$$

U_x, U_y, U_z are the components of the mean pore velocity $\mathbf{U}$. z_1, z_2, z_3 are random numbers issued from a uniform distribution between -1 and 1.

Particle Movement Inside One Finite Element

The mixed finite element method give the Darcy velocity in each element E. By dividing the fluxes by the porosity, one obtains the effective velocity of the

fluid particle given by

$$\mathbf{U}_E = \sum_{i=1}^{6} Q_i^{'} \mathbf{w}_i \tag{25}$$

where $Q_i^{'} = Q_i/\theta$, θ is the effective porosity, Q_i is the flux through each side A_i of the element E (positive for cell outflow), and $\mathbf{w}_i$ is the Raviart–Thomas basis functions.

The Raviart–Thomas basis functions in an cubic element of size $lx \times ly \times lz = V$, have the following expressions (u, v, w are the local coordinates in the element) (Fig. 1):

$$\begin{aligned} \mathbf{w}_1 &= \begin{pmatrix} \frac{u}{V} \\ 0 \\ 0 \end{pmatrix} \quad \mathbf{w}_2 = \begin{pmatrix} \frac{u-lx}{V} \\ 0 \\ 0 \end{pmatrix} \quad \mathbf{w}_3 = \begin{pmatrix} 0 \\ \frac{v}{V} \\ 0 \end{pmatrix} \\ \mathbf{w}_4 &= \begin{pmatrix} 0 \\ \frac{v-ly}{V} \\ 0 \end{pmatrix} \quad \mathbf{w}_5 = \begin{pmatrix} 0 \\ 0 \\ \frac{w}{V} \end{pmatrix} \quad \mathbf{w}_6 = \begin{pmatrix} 0 \\ 0 \\ \frac{w-lz}{V} \end{pmatrix} \end{aligned} \tag{26}$$

The advective particle displacement is then calculated by simply integrating the expression (14). In the x direction the particle velocity can be writen as

$$\begin{aligned} U_x(t) &= \left[\frac{Q_1^{'} + Q_2^{'}}{V} \right] \left[x(t) - x_{i-1/2} \right] - \frac{Q_2^{'}}{ly \times lz} \\ &= \left[\frac{U_{x_{i+1/2}} - U_{x_{i-1/2}}}{lx} \right] \left[x(t) - x_{i-1/2} \right] + U_{x_{i-1/2}} \end{aligned} \tag{27}$$

We note by $U_{x_{i-1/2}}$ (respectively $U_{x_{i+1/2}}$) the mean pore velocity at $u = 0$ (respectively $u = lx$) in the element where the particle is located (which is indeed $Q_2^{'}/(ly \times lz)$ (respectively $-Q_1^{'}/(ly \times lz)$)).

After integrating, one obtains

$$x(t + \delta t) = x_{i-1/2} + (1/A_x)\left[U_x(t) \exp(A_x \delta t) - U_{x_{i-1/2}} \right] \tag{28}$$

The spatial derivatives of the dispersion coefficients are calculated within each element according to the velocities and their own derivatives

$$\frac{\partial U_x}{\partial X} = \frac{U_{x_{i+1/2}} - U_{x_{i-1/2}}}{lx} \quad \text{and} \quad \frac{\partial U_x}{\partial Y} = \frac{\partial U_x}{\partial Z} = 0 \tag{29}$$

The derivatives of the dispersion coefficients are thus reduced to the following expressions:

$$
\begin{aligned}
\frac{\partial D_{xx}}{\partial X} &= U_x \frac{\partial U_x}{\partial X}\left[\alpha_{\mathrm{L}}\left(\frac{2}{U}-\frac{U_x^2}{U^3}\right)-\alpha_{\mathrm{T}}\frac{U_y^2+U_z^2}{U^3}\right]\\
\frac{\partial D_{xy}}{\partial Y} &= (\alpha_{\mathrm{L}}-\alpha_{\mathrm{T}})\left[\frac{\partial U_y}{\partial Y}\frac{U_x}{U}-\frac{U_x U_y^2}{U^3}\frac{\partial U_y}{\partial Y}\right]\\
\frac{\partial D_{xz}}{\partial Z} &= (\alpha_{\mathrm{L}}-\alpha_{\mathrm{T}})\left[\frac{\partial U_z}{\partial Z}\frac{U_x}{U}-\frac{U_x U_z^2}{U^3}\frac{\partial U_z}{\partial Z}\right]\\
\frac{\partial D_{yy}}{\partial Y} &= U_y \frac{\partial U_y}{\partial Y}\left[\alpha_{\mathrm{L}}\left(\frac{2}{U}-\frac{U_y^2}{U^3}\right)-\alpha_{\mathrm{T}}\frac{U_x^2+U_z^2}{U^3}\right]\\
\frac{\partial D_{yx}}{\partial X} &= (\alpha_{\mathrm{L}}-\alpha_{\mathrm{T}})\left[\frac{\partial U_x}{\partial X}\frac{U_y}{U}-\frac{U_y U_x^2}{U^3}\frac{\partial U_x}{\partial X}\right]\\
\frac{\partial D_{yz}}{\partial Z} &= (\alpha_{\mathrm{L}}-\alpha_{\mathrm{T}})\left[\frac{\partial U_z}{\partial Z}\frac{U_y}{U}-\frac{U_y U_z^2}{U^3}\frac{\partial U_z}{\partial Z}\right]\\
\frac{\partial D_{zz}}{\partial Z} &= U_z \frac{\partial U_z}{\partial Z}\left[\alpha_{\mathrm{L}}\left(\frac{2}{U}-\frac{U_z^2}{U^3}\right)-\alpha_{\mathrm{T}}\frac{U_x^2+U_y^2}{U^3}\right]\\
\frac{\partial D_{zx}}{\partial X} &= (\alpha_{\mathrm{L}}-\alpha_{\mathrm{T}})\left[\frac{\partial U_x}{\partial X}\frac{U_z}{U}-\frac{U_z U_x^2}{U^3}\frac{\partial U_x}{\partial X}\right]\\
\frac{\partial D_{zy}}{\partial Y} &= (\alpha_{\mathrm{L}}-\alpha_{\mathrm{T}})\left[\frac{\partial U_y}{\partial Y}\frac{U_z}{U}-\frac{U_z U_y^2}{U^3}\frac{\partial U_y}{\partial Y}\right]
\end{aligned}
\tag{30}
$$

When a particle goes from one element to the adjacent one, we apply the algorithm described hereafter. In a nonuniform flow, velocity is not derivable at the interface of two adjacent elements. Computing dispersion coefficient derivatives by using a finite difference approach would yield erroneous values.

Particles Transfer Across a Discontinuity

In a nonhomogeneous medium, as in the case of layered aquifers, the abrupt variation of the velocity field makes the calculation of the additional term problematic. To overcome this difficulty, two approaches have been proposed: the "reflecting barrier" approach and the interpolation technique.

In the literature, we found four authors who have already addressed this problem and tried to give different solutions. In order to illustrate the different

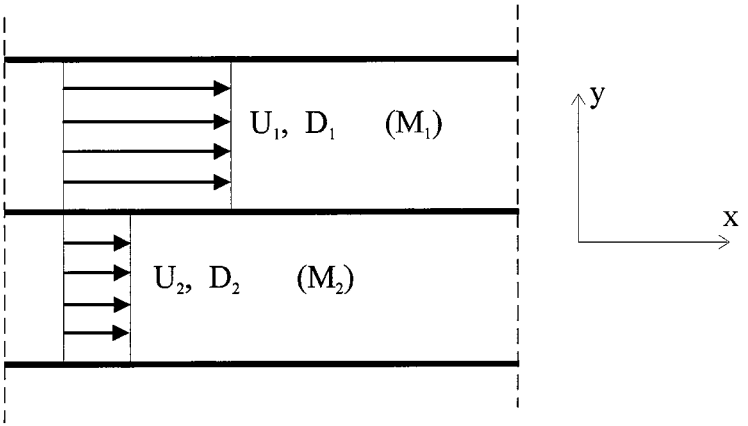

Figure 2. Schematic presentation of a layered aquifer.

approaches, let us study the case of a layered aquifer in which the flow is parallel to the layers and then we will study also the transfer in the perpendicular direction (Fig. 2).

The upper medium (M_1) is a high dispersive medium and the lower (M_2) is a low dispersive one.

The following three methods are reflecting-barrier approaches.

Uffink (1983) was probably the first who introduced the idea of a semireflecting barrier at the interface. He suggested that a part of the set of particles going from M_1 to M_2 must be reflected. This part is given by a probability of crossing the barrier defined by

$$P_u = \frac{\sqrt{D_{Y1}} - \sqrt{D_{Y2}}}{\sqrt{D_{Y1}} + \sqrt{D_{Y2}}} \tag{31}$$

where D_{Y1} is the transverse dispersion coefficient in the upper medium and D_{Y2} is the transverse dispersion coefficient in the lower medium.

Ackerer (1985) suggested another method. It consists in breaking up the particle jump through the interface, into two jumps. Let us consider that a particle jump duration be Δt. This jump is broken into two jumps, the first one takes the particle to the interface and it lasts Δt_1. This jump has the statistic properties of the first medium. The second jump starts at the interface with the statistic properties of the second medium and it lasts $\Delta t_2 = \Delta t - \Delta t_1$.

Cordes, Daniels, and Rouve (1991) went back to Uffink's idea (semireflecting barrier), but changed the probability for a particle to be reflected. They suggested

$$P_c = \frac{\sqrt{D_{Y1}} - \sqrt{D_{Y2}}}{\sqrt{D_{Y1}}} \tag{32}$$

The last approach is based on an interpolation technique presented by Labolle, Fogg, and Tompson (1996), and Labolle, Quastel, and Fogg (1998), which consists in interpolating velocities in the dispersion tensor in order to smooth the dispersion tensor in the vicinity of the interface to eliminate discontinuities. However, as mentioned by the authors, in order to attain the convergence to the true solution, this method requires convergence in time step as well as in the spatial discretization associated to the interpolation scheme.

To assess those different methods, we have used each of them to simulate a tracer transport in a bistrata aquifer (Labolle, Fogg, and Tompson, 1996). The same number of particles were injected in each layer. In this problem, a correct modeling technique will maintain a uniform particle number density in each strata, that is, $N_1/N_2 = 1$, where N_1 and N_2 are the particle numbers in each strata.

As shown in Labolle, Fogg, and Tompson (1996), using no correction fails to obtain uniform number density. In the following, we will compare results obtained with the four mentioned methods. To incorporate the technique of Labolle and coauthors, we linearly interpolate the diffusion coefficient through a unit length across the interface.

Tables 1 and 2 show the evolution of the number of particle ratios in the layers versus the dispersion coefficient values for each method. We test these methods with two simulation durations using two time steps $\Delta t = 0.005$ and $\Delta t = 0.5$. For the simulation duration of 500 time units, a time step of 0.005 gives good results for all methods (for the different ratios of dispersion coefficients). But a time step of 0.5 does not allow one to achieve an acceptable convergence for the four methods. For the simulation duration of 10,000 time units, neither time step (0.5 and 0.005) attains a satisfactory convergence with all methods.

This study shows that for all methods, the time step has to be adapted to the time duration of the simulation: in order to achieve convergence, we have to decrease the time step when the time duration increases.

A detailed analysis led us to think that the jump splitting up principle is a good way to approach reality, but since the particle is at the interface, the probability that it goes into one medium or another is not the same as is indicated in Cordes, Daniels, and Rouve (1991). Here we shall calculate the probability P_1 and $P_2 (P_2 = 1 - P_1)$ that the particle goes into one medium or another.

Let the dispersion displacement of a particle in the transversal direction be equal to

$$L_Y = z\sqrt{6D_Y \Delta t} \tag{33}$$

where z is a random number following a uniform distribution between -1 and 1 and D_Y is the dispersion coefficient in the y direction. In the homogeneous medium case, the value of particle displacements in the y direction would be uniformly distributed between $-\sqrt{6D_Y \Delta t}$ and $\sqrt{6D_Y \Delta t}$.

Table 1. Comparison in Ratios of Particle Numbers (N_1/N_2) on Either Side of Discontinuity in D for Different Alternative Techniques to Conserve Mass for a Simulation Duration of 500 Time Units for Two Time-Steps Δt

Time = 500 time unit (D_1/D_2)	Cordes		Uffink		Ackerer		Labolle	
	$\Delta t = 0.005$	$\Delta t = 0.5$	$\Delta t = 0.005$	$\Delta t = 0.5$	$\Delta t = 0.005$	$\Delta t = 0.5$	$\Delta t = 0.005$	$\Delta t = 0.5$
2.50	0.99	0.87	0.98	0.70	0.95	0.70	0.93	0.55
5.00	0.96	0.80	0.95	0.57	0.96	0.65	0.93	0.42
7.50	0.99	0.69	0.96	0.57	0.93	0.56	0.92	0.38
10.00	0.95	0.69	0.93	0.58	0.96	0.65	0.92	0.33
12.50	0.98	0.71	0.95	0.55	0.92	0.59	0.89	0.28
15.00	0.93	0.68	0.95	0.51	0.96	0.55	0.86	0.31
17.50	0.97	0.71	0.94	0.50	0.94	0.54	0.90	0.27
20.00	0.97	0.66	0.94	0.51	0.95	0.53	0.91	0.25
500.00	0.98	0.79	0.95	0.56	0.94	0.47	0.90	0.17

Table 2. Comparison in Ratios of Particle Numbers (N_1/N_2) on Either Side of Discontinuity in D for Different Alternative Techniques to Conserve Mass for a Simulation Duration of 10,000 Time Units for Two Time-Steps Δt

Time = 10,000 time unit (D_1/D_2)	Cordes		Uffink		Ackerer		Labolle	
	$\Delta t = 0.005$	$\Delta t = 0.5$	$\Delta t = 0.005$	$\Delta t = 0.5$	$\Delta t = 0.005$	$\Delta t = 0.5$	$\Delta t = 0.005$	$\Delta t = 0.5$
2.50	0.89	0.68	0.86	0.52	0.87	0.66	0.79	0.39
5.00	0.91	0.55	0.82	0.40	0.87	0.43	0.67	0.20
7.50	0.85	0.49	0.76	0.32	0.75	0.38	0.61	0.13
10.00	0.80	0.47	0.80	0.30	0.81	0.30	0.59	0.10
12.50	0.87	0.40	0.74	0.23	0.77	0.27	0.58	0.07
15.00	0.83	0.41	0.74	0.23	0.79	0.27	0.57	0.06
17.50	0.81	0.41	0.73	0.23	0.78	0.25	0.56	0.06
20.00	0.88	0.34	0.73	0.20	0.76	0.23	0.57	0.05
500.00	0.82	0.21	0.72	0.13	0.69	0.12	0.51	0.01

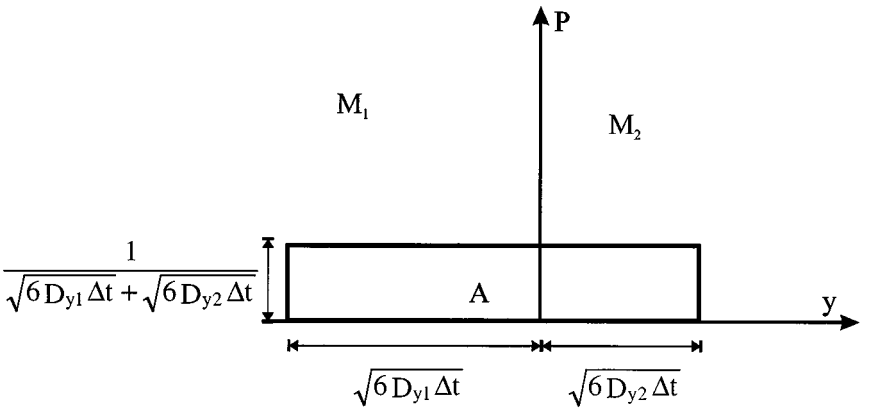

Figure 3. Probability distribution of particle dispersion jumps starting at the interface of the two layers.

In the nonhomogeneous medium case, the value of particle displacements in the y direction would be uniformly distributed between $-\sqrt{6\,D_{Y1}\,\Delta t}$ and $\sqrt{6\,D_{Y2}\,\Delta t}$.

To respect the uniform distribution (Fig. 3) of particle displacements in the whole area (A) of possible displacements, the probability that a particle goes into mediums M_1 and M_2 is respectively

$$P_1 = \frac{\sqrt{D_{Y1}}}{\sqrt{D_{Y1}} + \sqrt{D_{Y2}}} \quad \text{and} \quad P_2 = 1 - P_1 = \frac{\sqrt{D_{Y2}}}{\sqrt{D_{Y1}} + \sqrt{D_{Y2}}} \tag{34}$$

Finally, programming this method is not difficult; after splitting up the jump, the particle is at the interface and then one draws a random number R from a uniform distribution between 0 and 1: if $R < P_1$, the particle goes into the M_1 medium, else it goes into the M_2 medium. This algorithm must be applied whether the particle comes from one side of the interface or the other. It must also be applied when a particle goes from one element to the adjacent one, because the tangential velocity unit vector is not continuous from one element to the other. Table 3 clearly shows that the new method is the only accurate solution of the problem for any ratio of dispersion coefficients and without any big difficulties of convergence in time step.

MODEL VALIDATION

To validate the model we have simulated a tracer experiment in an heterogeneous medium performed on a 3D laboratory model (Fig. 4). The porous medium is 5.6 m in length, 1 m in width, and 0.8 m in depth. It is filled up with three different kinds of sand disposed in eight layers of randomly placed parallelepipeds

Table 3. Comparison in Ratios of Particle Numbers (N_1/N_2) on Either Side of Discontinuity in D for the New Technique to Conserve Mass for a Simulation Duration of 500 and 10,000 Time Units for Two Time-Steps Δt

	Time = 500		Time = 10,000	
D_1/D_2	$\Delta t = 0.005$	$\Delta t = 0.5$	$\Delta t = 0.005$	$\Delta t = 0.5$
2.50	1.00	1.01	1.06	1.03
5.00	1.00	1.02	0.97	1.02
7.50	1.00	0.98	1.05	1.03
10.00	1.00	1.02	1.00	1.06
12.50	1.00	0.96	1.04	1.01
15.00	1.01	1.07	0.98	0.99
17.50	1.00	0.99	0.99	0.99
20.00	1.01	1.02	0.99	1.00
500.00	1.01	1.02	1.02	1.00

of $0.4 \times 0.1 \times 0.1$ m^3. Figure 5 shows the distribution of sand blocks in the eight layers of the porous medium. Each layer is different from another. Sodium chloride is used at low concentration as a tracer because of its conductivity feature and to avoid density contrast effect. The concentration measuring setup consists in 352 conductivity cells installed in the porous medium (Ruch, Ackerer, and Guterl, 1992).

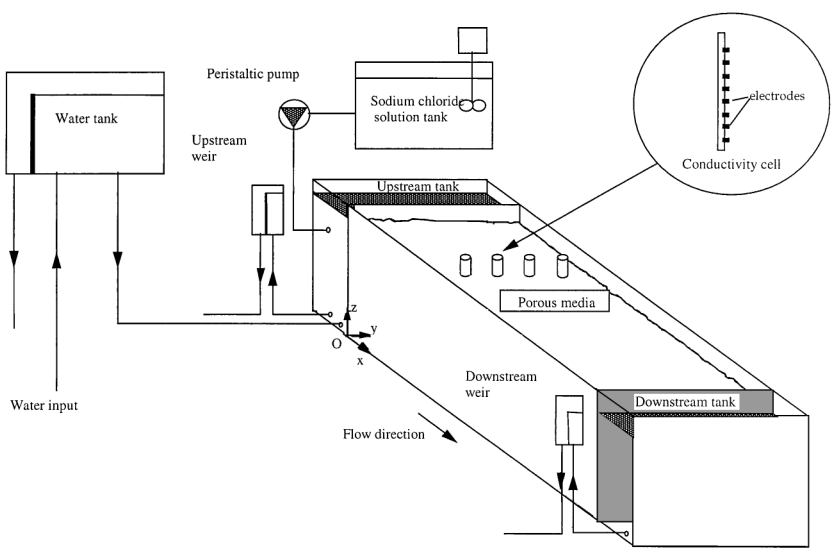

Figure 4. Schema of the laboratory model.

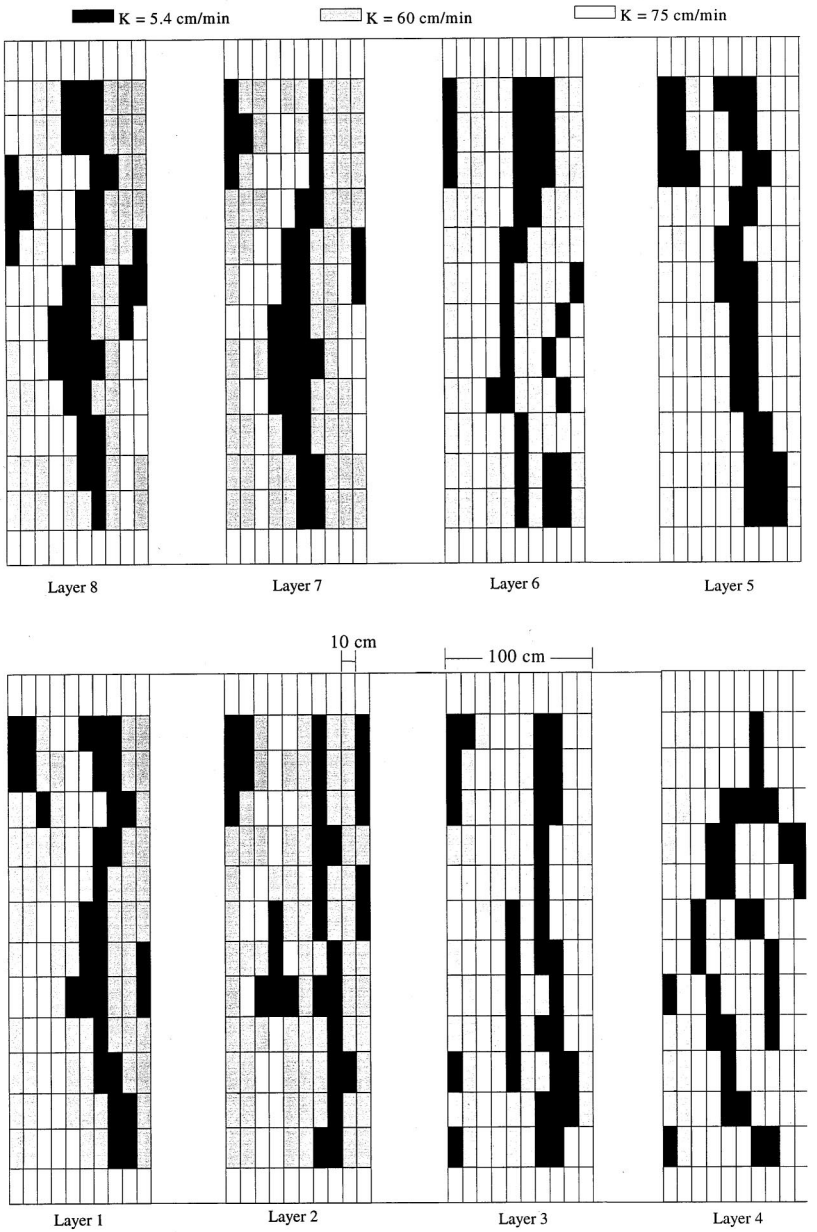

Figure 5. View of the distribution of sand blocks in the eight layers of the porous medium.

Hydraulic conductivities are $k_1 = 75$ cm/min, $k_2 = 60$ cm/min, and $k_3 = 5.4$ cm/min. These values were measured on laboratory samples of sand. The mean hydraulic gradient in the longitudinal direction is $J = 2.03 \times 10^{-2}$. Longitudinal dispersivity is $\alpha_L = 3$ mm and transversal dispersivity is $\alpha_T = 0.3$ mm. The porosity is $\varepsilon = 0.38$. The upstream tank ($x = 0$ cm) is used as pollution source. Sodium chloride is injected continuously in the upstream tank. The concentration breakthrough in the upstream tank is given by $C(t) = C_{max}(1 - e^{-\beta t})$, where $C_{max} = 1.08$ g/L and $b = 0.0476$. The domain was discretized into a regular parallelepipedic mesh. 17,280 elements were used (54 in x, 20 in y, and 16 in z direction). Each sand block was discretized into 16 elements.

Two simulations have been performed, the first one with and the other one without taking into account the corrective term. Figure 6 shows isoconcentration surfaces obtained from the two simulations. The figure clearly shows that neglecting the corrective term yields dramatic results. Unrealistic high concentrations are observed in low hydraulic conductivity regions (low dispersion). We show here the absolute necessity to take into account the corrective term. Figures 8 and 10 compare measured and simulated concentration in the fifth (at $z = 45$ cm, Fig. 7)

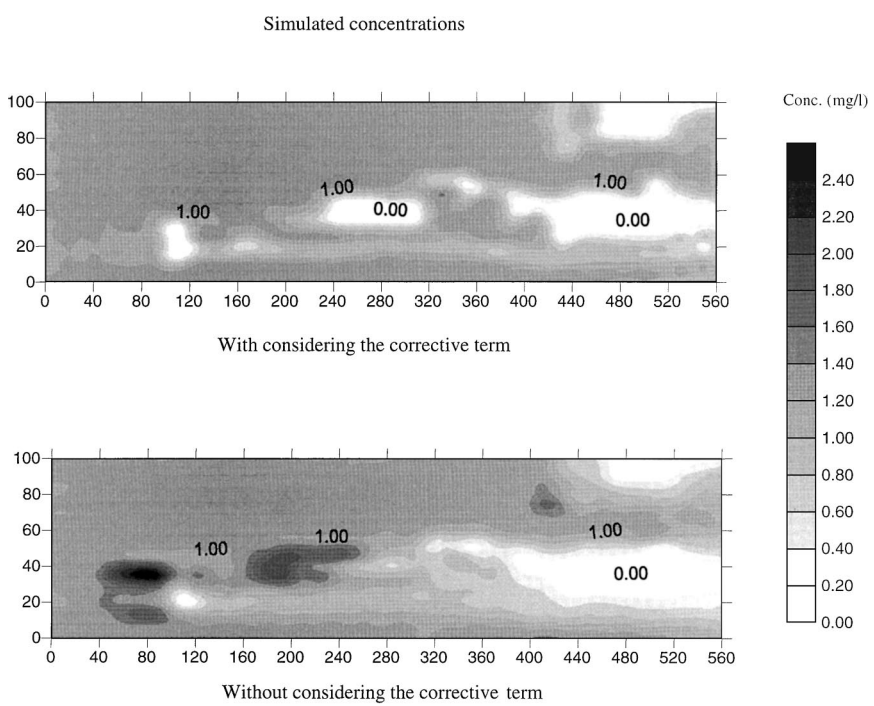

Figure 6. Isoconcentration surfaces obtained with and without taking into account the corrective term.

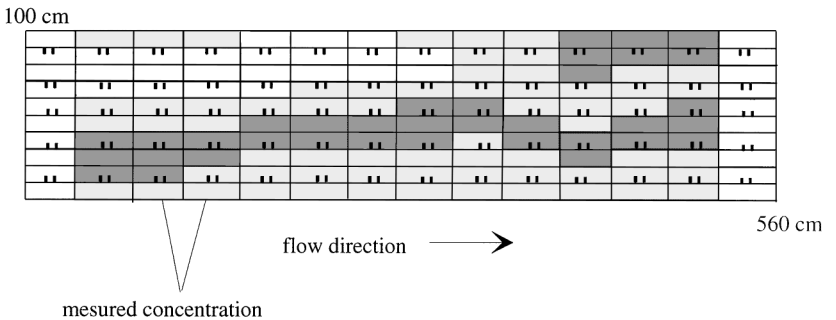

Figure 7. A horizontal section of the modeled domain at $z = 45$ cm (Layer 5).

and seventh (at $z = 65$ cm, Fig. 9) layer. It shows an acceptable agreement between measured and computed concentrations. Simulated isoconcentration surfaces are slightly different from measured isoconcentration on Figs. 7 and 8. Some differences can be explained by the permeability variability resulting from the manual

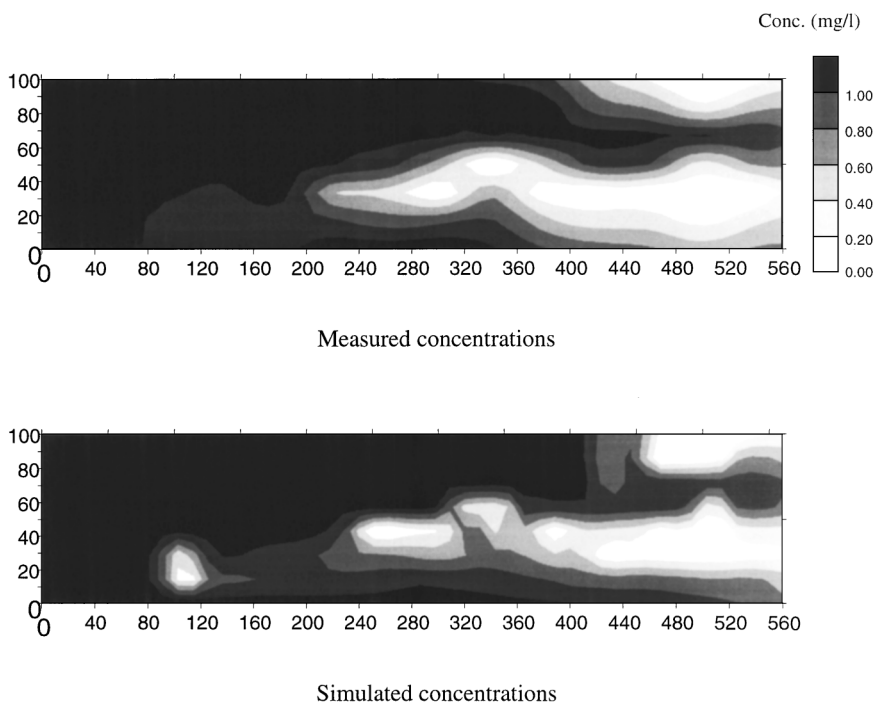

Figure 8. Comparison between measured and simulated concentrations for the horizontal section $z = 45$ cm, at time $t = 232$ min.

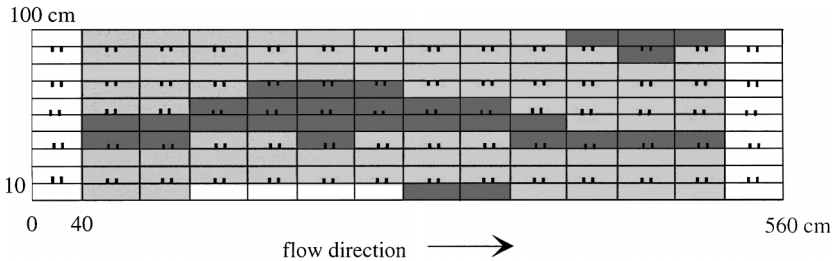

Figure 9. A horizontal section of the modeled domain at $z = 65$ cm (Layer 7).

packing of the sand. Some others can be explained by the variability of the shape of the sand blocks, which are not perfect parallelepiped because the grid we have used for the filling was too supple. Moreover we have used the elements of the mesh to represent the distribution of the concentration in the medium (1080 elements in each layer) while we have only used the measurement cells which are at the number of 70.

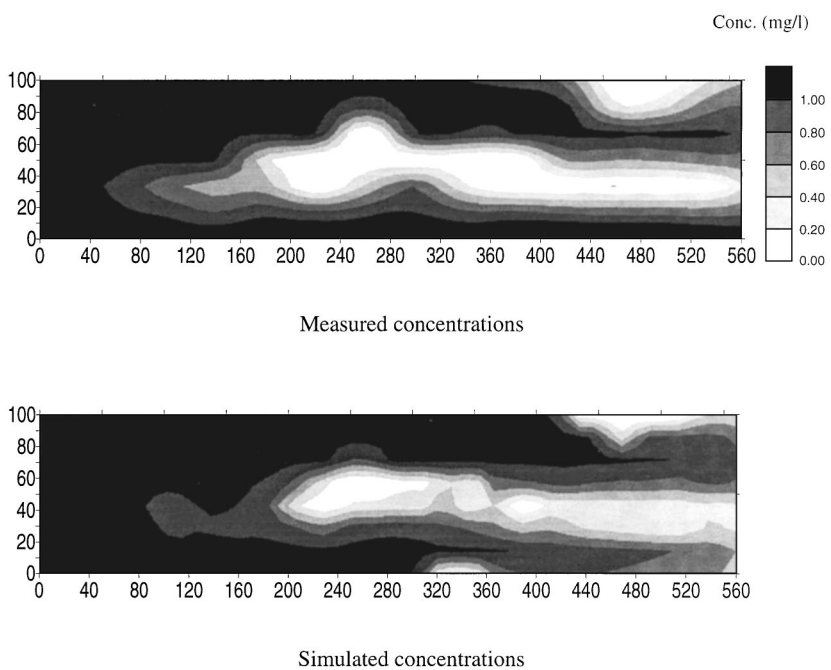

Figure 10. Comparison between measured and simulated concentrations for the horizontal section $z = 65$ cm, at time $t = 232$ min.

To conclude with that simulation of Marceau's experiment, an acceptable match between measurement and simulation is achieved everywhere.

CONCLUSION

At field scale and especially in heterogeneous media, solute transport is always a 3D phenomenon. Therefore an efficient groundwater quality modeling must be 3D as well. The random-walk method is a good alternative to classical techniques as finite difference and finite elements, which suffer from numerical diffusion at high Peclet numbers. But classical random-walk models are not efficient in simulating mass transport in heterogeneous media because if the additional term is not correctly taken into account, particle accumulation can occur in low dispersion areas. The new method developed in this study allows the conservation of the particle fluxes between high and low dispersive regions. Table 3 (compared to Tables 1 and 2) shows the efficiency of this method and its superiority on other algorithms commonly used. The 3D code, developed in this study takes into account the new algorithm which has been extended to the three directions of space. The code has been verified on hand of a 3D laboratory experiment. Comparisons between simulated and measured values have shown satisfactory results.

In this paper it is also shown that a 3D physical laboratory model is a very useful tool in validating numerical models before their use at field scale and also to improve our understanding in mass transfer in porous media.

REFERENCES

Ackerer, Ph., 1985, Propagation d'un Fluide en Aquifère Poreux Saturé en Eau. Prise en Compte et Localisation des Hétérogénéités par des Outils Théoriques et Expérimentaux: Doctoral dissertation, Université Louis Pasteur de Strasbourg, France, 102 p.

Bear, J., 1979, Hydraulics of groundwater: McGraw-Hill, New York, 569 p.

Brezzi, F., and Fortin, M., 1991, Mixed and hybrid finite element methods: Springer, New York, 350 p.

Chavent, G., and Roberts, J. E., 1991, A unified physical presentation of mixed, mixed hybrid finite elements and standard finite difference approximations for the determination of velocities in water flow problems: Adv. Water Resour., v. 14, no. 6, p. 349–355.

Cordes, C., Daniels, H., and Rouve, G., 1991, A new very efficient algorithm for particle tracking in layered aquifers, *in* Bensari, D., Brebbia, C. A., and Ouazar, D. eds., 2nd international conference on computer methods and water resources, Rabat, Morocco, Computational Mechanics Publications, WIT Press, p. 41–55.

Gardiner, C. W., 1985, Handbook of stochastic methods for physics, chemistry and the natural sciences, 2nd edn.: Springer, Berlin, 434 p.

Itô, K., 1951, On stochastical differential equations, Vol. 4: American Mathematical Society, New York, p. 289–302.

Kinzelbach, W., 1986, Groundwater modeling: Introduction with sample programs in Basic: Developments in Water Science, 25th edn.: Elsevier, Amsterdam, 333 p.

Labolle, E. M., Fogg, G. E., and Tompson, A. F. B., 1996, Random-walk simulation of transport in heterogeneous porous media: Local mass conservation problem and implementation methods: Water Resour. Res., v. 32, no. 3, p. 583–593.

Labolle, E. M., Quastel, J., and Fogg, G. E., 1998, Diffusion theory for transport in porous media: Transition probability densities of diffusion processes corresponding to advection–dispersion equations: Water Resour. Res., v. 34, no. 7, p. 1685–1693.

Mosé, R., Siegel, P., Ackerer, Ph., and Chavent, G., 1994, Application of the mixed hybrid finite element approximation in a groundwater flow model: Luxury or necessity?: Water Resour. Res., v. 30, no. 11, p. 3001–3012.

Pinder, G. F., and Gray, W. G., 1977, Finite element simulation in surface and subsurface hydrology: Academic Press, New York, 295 p.

Raviart, P. A., and Thomas, J. M., 1977, A mixed hybrid finite element method for the second order elliptic problems, in mathematical aspects of the finite element method, lecture notes in mathematics: Springer, New York.

Ruch, M., Ackerer, Ph., and Guterl, P., 1992, A computer driven setup for mass transfer in porous media: *in* proceedings of Hydrocomp'92 international conference on interaction of computational methods and measurements in hydraulics and hydrology, Budapest, p. 419–426.

Semra, K., 1994, Modelisation tridimensionnelle du transport d'un traceur en milieu poreux saturé hétérogène: Evaluation des théories stochastiques: Doctoral dissertation, Université Louis Pasteur de Strasbourg, France, 125 p.

Uffink, G. J. M., 1985, A random-walk method for the simulation of macrodispersion in a stratified aquifer: *in* proceedings of IAHS symposia, IUGG 18th general assembly, Hamburg, IAHS Publication, v. 65, p. 26–34.

Uffink, G. J. M., 1990, Analysis of dispersion by the random walk method: Doctoral dissertation, Delft University, The Netherlands, 150 p.